

PALSAR ScanSAR Interferometry Using The Modified Full Aperture Processing

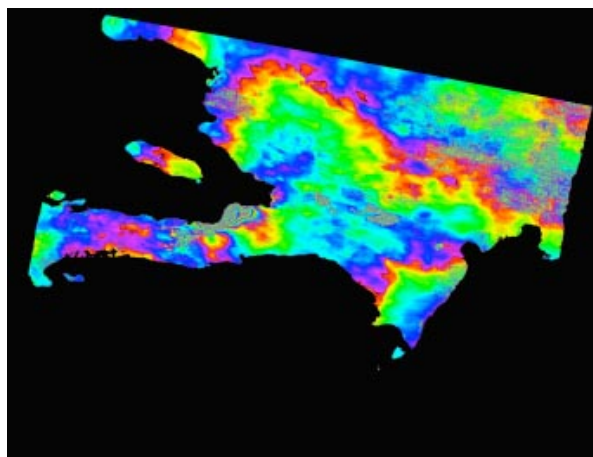
SHIMADA, Masanobu^{1*}

¹Japan Aerospace Exploration Agency

ScanSAR processing is represented by a Specan SAR and a full aperture SAR, latter of which creates the interpolated raw data from the intermittently transmitted and received signal and zero padding based on the transmit/receive timing. Here, we propose a modified full aperture ScanSAR imaging that performs the azimuth correlation for the azimuthally resampled range compressed data using the referenced PRF-value. This method allows the creation of the full swath SLC and allows the co-registration easily in the InSAR processing. We have tested the sensitivity of the ScanSAR interferometry for various types of the targets, disaster, desert, forest, and evaluated the coherence dependence on the beam synchronization.

At the operation of the PALSAR ScanSAR imaging (amplitude), we adopted the SPECAN SAR processing algorithm for the PALSAR wide-swath (ScanSAR) imaging [1][2]. The Specan method [1] minimized the three representative problems that the ScanSAR faces, i.e., scalloping, azimuth ambiguity, and inter-scan banding. While the SPECAN algorithm exceeds the full aperture SAR processing in that no out-of-use area exists, i.e., synthetic aperture length, in the processing phase, the phase continuity over the contiguous burst seems to be difficult. The PALSAR first Specan ScanSAR-ScanSAR interferometry was tested [3]. We first compared the strip InSAR and Specan InSAR for the simulated ScanSAR from the strip. This does not generate any discontinuity between the images. Second image is the ScanSAR result for the Saharan Desert area, which shows the relatively high coherence and the very good fringe. However, the problem was the discontinuity of the fringes. Third example is the ScanSAR of the south of the Tanzania area. This also shows high coherence and good fringes. But the problem was the phase discontinuity. Thus, in this paper, we propose a modified full aperture ScanSAR processing and its application to the ScanSAR Interferometry.

Keywords: SAR, ScanSAR InSAR, Surface Deformation, ALOS



Evaluation for detection capability of ground subsidence by InSAR time series analysis

MIYAHARA, Basara^{1*}, YAMANAKA, Masayuki¹, KOBAYASHI, Tomokazu¹

¹Geospatial Information Authority of Japan

Geospatial Information Authority of Japan (GSI) has been monitoring ground subsidence at 17 areas in Japan with SAR Interferometry (InSAR) analysis of ALOS/PALSAR. The subsidence is estimated by stacking process of several InSAR images, which averages and reduces noise included in the images. We evaluated detection capability of the stacking method by comparing subsidence measured by leveling. The result shows that the subsidence detected by both methods is consistent within about 1cm at Kujukuri Plain, Tsugaru Plain and Niigata Plain. In order to evaluate detection capability of ground subsidence by InSAR time series analysis, we estimate subsidence by InSAR time series analysis at still subsiding Tsugaru Plain, and compare the result with those by leveling and stacking method.

Keywords: SAR Interferometry, Time series analysis, Ground subsidence, StaMPS, ALOS, PALSAR

Three dimensional water vapor distribution based on InSAR data during Seinoh heavy rain on 2 September 2008

KINOSHITA, Youhei^{1*}, SHIMADA, Masanobu², FURUYA, Masato¹

¹Natural History Sci. Hokkaido Univ., ²Earth Observation Research Center, Japan Aerospace exploration Agency

Interferometric Synthetic Aperture Radar (InSAR) phase signals allow us to map the Earth's surface deformation, but are also affected by earth's atmosphere. In particular, the spatiotemporal heterogeneity of water vapor near the surface causes unpredictable phase changes in InSAR data and prevents us from detecting few centimeters of crustal deformation. However, InSAR can provide us with a spatial distribution of precipitable water vapor with unprecedented spatial resolution in the absence of deformation signals and other errors (Fujiwara et al., 1998, Hanssen et al., 1999).

We generated the InSAR image from ALOS/PALSAR level 1.0 data acquired during the heavy rain on 2 September 2008 in Central Japan, so-called Seinoh heavy rain, and then we detected the localized signal which changed 120 mm in radar line-of-sight over a spatial scale on the order of 8 km. So far we have reported that; 1) the localized signal is likely to be an artifact of tropospheric propagation delay rather than that of either ground deformation or ionosphere, 2) comparing it with the 1 km weather radar rainfall intensity echo distribution, the small area with rainfall intensity greater than 80 mm/hr exists at the location of the signal in InSAR (Kinoshita et al., GSJ 2010, 2011 meeting, Kinoshita et al., 2011, JpGU). Here we report the estimated result of three dimensional water vapor distribution during the heavy rain based on the heavy rain-derived tropospheric delay signal in InSAR data with the ray tracing method (Hobiger et al., 2008). We used the GAMMA software for the InSAR analysis and the 10 m digital elevation model by GSI for the correction of topographic fringes.

The refractivity of earth's atmosphere is the function of pressure, temperature, and water vapor (Thayer, 1974). Therefore we estimated the three dimensional water vapor distribution to explain the localized signal in InSAR by at first setting the three dimensional field of pressure, temperature and water vapor around the localized signal at the SAR acquisition time, then modeling the tropospheric delay in InSAR with ray tracing. Here, since it is impossible to determine these three parameters uniquely from one refractivity without any constraint, and since the ray path of each pixel is parallel in InSAR, it is difficult to estimate these parameters by the inversion like GPS tomography (e.g. Seko et al., 2000). For these reasons, we assumed as a constraint that the values of pressure and temperature are same as the MSM data, and we only estimated the water vapor distribution, which is spatiotemporally variable and has large effect on the propagation delay, by trial and error. In this study we focus only on the localized signal in InSAR, and the region we estimate is 30 km square centered on the localized signal in the horizontal and 15000 m in the vertical.

As a result, we estimated that there is the dry region lower than 50 % in relative humidity above 5000 m altitude, and the large amount of water vapor higher than 90 % in relative humidity within 10 km square in the horizontal and from the surface to 9000 m in the vertical at the localized signal in InSAR. Calculating the zenith precipitable water vapor (PWV) from the estimated water vapor field, we found that the amount of PWV at the signal in InSAR is 12 mm higher than that around the signal, and the location of it is 3 km apart from the local maximum area of weather radar echo. Additionally, it seems that AMeDAS surface wind observation data shows the existence of the convergence zone at the signal in InSAR. This indicates that water vapor near the surface converges at the signal. For these reasons, the location of the dense water vapor area is markedly different from that of the maximum precipitation radar echo. This observation would represent that in the precipitation system for the heavy rain the actually precipitating area was 3 km distant from the area where the water vapor was flowing into.

Keywords: InSAR, Heavy rain, Ray tracing, Water vapor

Crustal deformation around 62-II crater of Tokachidake Volcano, central Hokkaido Japan, depicted by InSAR of ALOS/PALSAR

KOSHIROMARU, Takuma^{1*}

¹Inst. of Seismology and Volcanology, Hokkaido Univ.

Mt. Tokachi is an active volcano with an altitude of about 2077 m, located almost at the center of the Mt. Tokachi volcano group which aligns along northeast to southwest trend in the central Hokkaido. Since the beginning of the 20th century Mt. Tokachi has been repeating eruptions in 1926, 1962, and 1988-89 with an approximate recurrence period of 30 years. In the north-northwest part of Mt. Tokachi there are number of craters, i.e., Nokogiridake crater, Ground crater, Suribachi crater, Kitamukai crater, Tyuoh crater, and 62-II crater. Among them the 62-II crater was formed by the eruption in 1962 and also used by eruption in 1988-1989. GPS observations by Japan metrological agency and others revealed that an inflation around this crater is on-going. In this paper, we present ALOS/PALSAR interferometry results depicting deformation of crustal deformations of Tokachi volcano.

We used ALOS/PALSAR data taken during the period from 2006 to 2010. A total of 38 scenes (20 from ascending and 18 from descending orbits) were available for the analysis. From these raw data, we constructed interferograms for the pairs whose orbit baseline lengths are reasonably short and temporal baseline is sufficiently long. Firstly we examined only nterferograms with the highest quality. From the first analysis we excluded interferotrams where the paired observations were carried out to the snow covered ground and/or ones having large noises caused by the atomosphere. Those errors are caused by the heterogeneous microwave propagation through the ionosphere and troposphere. An example of such high-quality data was taken with the pair on June 30, 2008 and October 3, 2009. We can recognize a localized phase change pattern around 62-II crater, suggesting an localized inflation around the crater which is in good agreement with the GPS results.

Then we stacked relatively good interferograms with small noises scattering over the observed region. In many cases those noises are in good correlation of the trend of the rugged topography of the mountainous region suggesting existence of propagation heterogeneity in the data, which expected to be of random nature. The stacked interferogram also depicts a localized phase change around 62-II crater which is in good agreement with the highest quality interferograms as well as GPS data. We do not find any other significant fringes (phase changes) around the other craters. By fitting of Mogi model for our InSAR results, a source was estimated below the 62-II crater at the depth of about 1 km.

In this study, whole InSAR processing was performed using SIGMA-SAR by Dr. Masanobu Shimada of JAXA-ERO. We used 10m-mesh Digital Elevation Model compiled by the Geospatial Information Authority of Japan (GSI). PALSAR level 1.0 data were provided from the Earthquake and Volcano Working Groups as well as PIXEL (PALSAR Interferometry Consortium to Study our Evolving Land surface) under a cooperative research contract with JAXA (Japan Aerospace Exploration Agency). The ownership of PALSAR data belongs to METI (Ministry of Economy, Trade and Industry) and JAXA.

Keywords: InSAR, Crustal Deformation, Tokachidake, ALOS, PALSAR, Volcano

Analysis of crustal deformation due to the 2010 El Mayor-Cucapah Earthquake in Mexico using SAR data

OKAMOTO, Junichi^{1*}, HASHIMOTO, Manabu¹, FUKUSHIMA, Yo¹

¹DPRI, Kyoto University

El Mayor-Cucapah earthquake (Mw 7.2) occurred on April 4th, 2010, in Baja California, a region of high seismicity in association with the complex Pacific and North American plate boundary. Its hypocenter is located near a pull-apart basin and the tectonics in this area is very complex owing to distributed normal and conjugate strike-slip faults. In this study, we are going to reveal relationship between the generation process of co- and postseismic fault motions by detecting detailed co- and postseismic deformations by using ALOS/PALSAR and ENVISAT/ASAR data.

We detected range change of about 150cm in the vicinity of the source fault in the ascending co-seismic interferograms. However, we recognized disturbances of fringes in the vicinity of the northwestern part of the source fault and phase discontinuity at a separate fault off the main rupture. In the descending images, we can recognize many concentric fringes along the traces of northwestern part of the source fault, which suggest that local fault motion occurred in connection with the main rupture. In addition, the phase discontinuity is observed in the same area of the ascending interferograms. Therefore subsidiary faults off the main source fault may have generated local deformation during the main shock. We assumed a sufficiently large rectangular plane fault and estimated slip distributions on it. Right lateral strike slips with slight normal component were estimated, and its maximum slip of about 3.5m was obtained in the northwestern vicinity of the hypocenter and at a depth of 3-4km. The optimal dip angle was 68 degrees. While this model can explain the main feature of co-seismic deformation, the residuals in the vicinity of the northwestern part of the source fault are slightly larger than southeastern part. This suggests that it is difficult to explain these local deformations by estimated fault model.

During the postseismic period, about six months after the main shock, we recognized some signals in the northwestern part of the source fault in both ALOS and ENVISAT descending interferograms. Some profiles show range increases (movement to west or subsidence) up to 5cm. These displacements are observed on the west side of the source fault except at the northwestern edge. In addition, we recognized range increase of about 2.5cm in the vicinity of the other faults about 10km southwest of the source fault. This suggests that other faults, which did not slip during co-seismic period, could have moved during the postseismic period. We estimated postseismic slip distributions on the estimated co-seismic fault model. Reverse dip-slip components were dominant in the northwestern part. However this reverse dip-slip is inconsistent with slip during the mainshock in this region, and this model could not explain observed data well. Therefore observed postseismic deformations could have been generated by other factors.

Here, we assumed models with five faults dipping to southwest to explain the postseismic deformations. After trial and errors, we could find a model that can explain the observed phase variations and is consistent with co-seismic fault model which includes slightly normal component. This suggests that subsidiary faults in the vicinity of the source fault moved after the main shock as a result of complex changes of the stress in the crust.

Keywords: SAR, interferometry, El Mayor-Cucapah earthquake, coseismic deformation, postseismic deformation, afterslip

2.5 Dimension Analysis of Ground Deformation in the Kyoto Basin and Osaka Plain Detected with SAR Interferometry

HASHIMOTO, Manabu^{1*}

¹DPRI, Kyoto University

We have been conducting an interferometry of SAR images acquired by ALOS/PALSAR and TerraSAR-X to reveal ground deformation and the configuration of basement of the Kyoto basin and the Osaka plain. We have analyzed PALSAR ascending images and applied a 2.5 dimension analysis to the stacked interferograms from both the ascending and descending orbits.

We analyzed 24 SAR images from the path 414 and frame 680 acquired during the period from October 8, 2006 to October 19, 2010. Pairs of images that have as short perpendicular baselines and long temporal intervals as possible were selected for interferometry. After that, interferograms were stacked to obtain average rate of line-of-sight (LOS) changes. During the interferometry, we applied flattening in order to reduce long-wavelength noise, which might have been originated by ionospheric disturbances. We used PALSAR images from descending orbit (path 65, frame 2920).

Last year, we detected LOS decrease in the southern part of Kyoto basin and LOS increase along the Arima-Takatsuki Tectonic Line (ATTL) from the analysis of descending images. Furthermore, analyses of TerraSAR-X images also gave similar results, which suggests that these observations revealed real ground deformations. In this study, we also recognized LOS decrease in southern part of Kyoto basin and LOS increase along the ATTL.

Then we applied 2.5 dimension analysis to these stacked interferograms to decompose LOS velocities in two directions into E-W and quasi-vertical components. Finally, we obtained about 1 cm/yr uplift in the southern part of Kyoto basin and 5 mm/yr subsidence along ATTL. In these areas, we did not recognize notable horizontal components, which suggests that they are purely uplift or subsidence. Interestingly, uplift in Kyoto is bounded by two active faults (Katagihara and Haibara faults). It is worth noting that more than 1 cm/yr subsidence were observed at the western edge of ATTL in the Toyonaka city. Other notable features are (1) subsidence in the reclaimed area on the coast of the Osaka Bay, (2) subsidence north of the Yodo River, and (3) subsidence west of the Osaka Prefectural Office.

The origin of these ground deformation remains hypothesis, but it is speculated that changes in groundwater table may affect the ground deformation in the Kyoto basin, since there is a big reservoir. Subsidence along ATTL may also be related to change in groundwater level and associated compaction of soil. One possibility is the postseismic effect of the 1995 Kobe earthquake, since the feature of the subsidence is quite similar to that observed during the postseismic period of the 2006 Mozambique earthquake.

PALSAR level 1.0 data were obtained from JAXA (Japan Aerospace Exploration Agency) under MEXT's (Ministry of Education, Culture, Sports, and Science and Technology) research project (Intensive Observation of the Uemachi Fault). The ownership of PALSAR data belongs to METI (Ministry of Economy, Trade and Industry) and JAXA. TerraSAR-X images were supplied by Pasco Ltd. under the Research Program by the Forum for the Application of SAR Technology. Copyright of TerraSAR-X images belongs to Infoterra GmbH.

Keywords: InSAR, ground deformation, Kyoto Basin, Osaka Plain, ground subsidence, Arima-Takatsuki Tectonic Line

Crustal Movements associated with the 2011 eruption of Shinmoe-dake detected by DInSAR and GPS

MIYAGI, Yosuke^{1*}, OZAWA, Taku¹, KOHNO, Yuhki¹

¹National Research Institute for Earth Science and Disaster Prevention

Shinmoe-dake in the Kirishima volcano group located in southwestern part of Japan started to erupt on January 19, 2011 and the eruption developed to Sub-Plinian and Vulcanian type eruptions on January 26 and 27. A generation of lava dome and its rapid growth within the crater were accompanied by succeeding explosive eruptions. The explosive phase ceased by the end of March. A magnitude of the 2011 eruption was large comparable to 1716-1717 eruptions that lasted for about one and half year, therefore it is necessary to take care for a while.

Although it is generally difficult to make a field observation in dangerous active volcanoes, a satellite remote sensing can make observations of even ongoing volcanoes periodically. Especially, SAR sensor is well-suited for monitoring of active volcanoes because it can penetrate ash clouds. Moreover, SAR data are applicable to use a DInSAR technique to detect crustal movement caused by magmatic activities. Around the Shinmoe-dake volcano area, there is a GPS network operated by GSI and NIED since before the 2011 eruption. This set of geodetic data from both DInSAR and GPS indicates pre-eruptive, co-eruptive, and post-eruptive deformation, and they are quite helpful to understand a condition of the volcano for each period and to anticipate future unrests. In this research, we use geodetic data from DInSAR and GPS to estimate and discuss about a volume change of the magma source associated with the 2011 eruption of Shinmoe-dake volcano.

Keywords: SAR, DInSAR, GPS, Shinmoe-dake, Crustal movement

Temporal change in the Shinmoe-dake crater detected by SAR analysis

OZAWA, Taku^{1*}, MIYAGI, Yosuke¹

¹NIED

In the 2011 Shinmoe-dake (Kirishima-yama) eruption, lava appeared in the crater, and the topography in the crater was changed significantly. We analyzed SAR images acquired by several satellites and revealed that lava in the crater had rapidly grown during January 29 until January 31. Its extrusion rate was estimated to 7.5 million m³/day, and volume of lava reached to 15 million m³ at January 31. After that, lava was covered by volcanic ejecta, and it seems that volume in the crater slightly increased from that of January 31, according to SAR images which were acquired in March.

A small eruption occurred on September 7 and has not been observed after that. To investigate change in the crater after the last eruption, we applied SAR interferometry using four RADARSAT-2 data which were acquired every 24 days from November 22. High coherences were obtained in and around the crater. Significant phase differences were obtained in the crater, indicating the sum of the phases due to the topographic change and surface deformation. So we divided it based on the assumption that deformation speed has been constant. Volume of ejecta accumulated in the crater (including lava) was estimated to 20 million m³, indicating that volume change from March was insignificant. Estimated surface deformation component indicates that the slant-range contraction has occurred; its speed was 5cm/24days. Assuming its slant-range change to be uplift, volume change rate is estimated to 275m³/day.

Keywords: Shinmoe, Kirishima, crater, SAR, deformation, lava

Crustal deformation around the Laguna del Maule caldera detected by PALSAR/InSAR

OZAWA, Taku^{1*}

¹National Research Institute for Earth Science and Disaster Prevention

Local deformations around volcanoes associated with the 2011 Tohoku Earthquake were found in our previous study (Ozawa and Fujita, submitted to JGR). To investigate if the similar deformation has occurred for other earthquakes, we are analyzing InSAR data for several areas. In this presentation, we present a result of the Laguna del Maule, Chile. The Laguna del Maule is a caldera with 15*25km width, located to east of seismic area of the 2010 Maule Earthquake (Mw8.8, 2010/2/27). Although there is no historical record of eruption, large deformation had been detected by InSAR. Applying InSAR using PALSAR data, we investigated crustal deformation for preseismic, coseismic, and postseismic periods. Due to disturbance by snow cover, sufficient coherence for deformation investigation was limited to pair of summer data. Now, we finished analyzing four interferometric pairs, (1)2007/2/12-2009/2/17, (2)2009/2/17-2010/2/20, (3)2010/2/20-2010/4/7, and (4)2010/4/7-2011/1/8. Obtained interferograms showed slant-range contractions, indicating inflation of volcano. Estimating source parameters of Mogi's model from interferograms of (1), (2), and (4), the source location was estimated to 2700m depth (b.s.l.) under the caldera. Simulated slant-range changes from the estimated model well explain observed ones. Volume changes were estimated to 54, 44, and 24 million m³, corresponding to rates of 27, 43, and 32 million m³/yr. Calculating slant-range change in 46 days from the averaged inflation rate (34 million m³/yr), it is roughly consistent with that from interferogram of (3). It suggests that significant inflation change didn't occur in the 2010 Maule Earthquake. However, this is a preliminary result, and then more detailed analysis is necessary.

Keywords: volcano, earthquake, deformation, SAR, Laguna del Maule

Surface deformation of Kuchinoerabujima volcano revealed by PS-InSAR time-series analysis

TANAKA, Akiko^{1*}, YAMAMOTO, Keigo²

¹Geological Survey of Japan, AIST, ²DPRI, Kyoto University

Kuchinoerabujima volcano is an active volcanic island located on the volcanic front of the Ryukyu island arc. Recent eruptive activities of Kuchinoerabujima volcano occurred at two active craters of Shindake and Furudake. Eruption was not observed for more than 30 years, however, seismic swarms were accompanied with radial outward pattern from the summit crater during January-June 2005, September 2006-January 2007, and September 2008-January 2009 (e.g., Saito and Iguchi, 2007). Ground displacements near the summit area of Shindake were also detected by interferometric SAR (InSAR) analysis using ALOS/PALSAR data (Yamamoto, 2009).

We report the result of an InSAR time-series analysis applied on data acquired over Kuchinoerabujima volcano. Persistent scatterer SAR interferometry (PS-InSAR) analysis using the StaMPS algorithm (Hooper et al., 2007) is applied to ALOS/PALSAR data. Both ascending and descending orbits, PS-InSAR analysis identified enough numbers of coherent pixels. The obtained line-of-sight (LOS) displacements showed rather complicated pattern compared with previous results. The obtained deformation near the summit area of Shindake was consistent with results of conventional InSAR and GPS. Also, it suggests another deformation source, which are not clearly accounted for previously.

Acknowledgements: PALSAR level 1.0 data are shared among PIXEL (PALSAR Interferometry Consortium to Study our Evolving Land surface), and provided from JAXA under a cooperative research contract with ERI, Univ, Tokyo. The ownership of PALSAR data belongs to METI (Ministry of Economy, Trade and Industry) and JAXA.

Keywords: PS-InSAR, time-series analysis, Kuchinoerabujima volcano, ground deformation, ALOS/PALSAR

Crustal deformation after the Iwate-Miyagi Nairiku earthquake deduced from PS-InSAR time series analysis

OHSHTA, Yuya^{1*}, OHTA, Yusaku¹, MIURA, Satoshi², DEMACHI, Tomotsugu¹, Kenji Tachibana¹, UMINO, Norihito¹

¹RCPEVE, Tohoku university, ²ERI, The University of Tokyo

The 2008 Iwate-Miyagi Nairiku (inland) earthquake occurred beneath the border between the Iwate and Miyagi prefectures in northeastern (NE) Japan, within Ou back-bone range (OBR) strain concentration zone [1] at 08:43 JST, 14 June 2008. Its focal mechanism is a reverse fault type with a W-NW to E-SE compressional axis. Ohta et al. [2] suggested that the coseismic fault plane is mainly west dipping based on the kinematic GPS analysis. Iinuma et al. [3] investigated the postseismic deformation deduced from the dense continuous and temporal GPS network. They found that the aseismic slip occurred at the shallower part of the coseismic slip and Dedana fault where did not slip during the mainshock rupture. Furthermore, Ohzono [4] found the long-term postseismic deformation in and around the focal area deduced from the continuous GPS data. She pointed out that this long-term postseismic deformation is caused by viscoelastic relaxation in lower crust or upper mantle. This model explains well the observed GPS data in far field. However, the simple viscoelastic model fail to explain the near field GPS data (e.g. [4, 5]). In this study, we apply InSAR time-series analysis by PS (Persistent Scatterer) method for investigation of long-term postseismic deformation near the focal area.

We applied StaMPS [6, 7] approach to the ALOS/PALSAR data obtained by the JAXA. In order to produce our interferograms, we processed a set of 12 descending orbit SAR images (Track 57, Frame 2830), acquired by the ALOS/PALSAR sensors from July 2008 to October 2010. In particular, SRTM4 Digital Elevation Model of the study area and precise orbital information were used for the interferograms generation. The master data image is acquired in September 3rd, 2009. We assumed the amplitude dispersion index (D_A) is as 0.4 that is threshold value defined by Ferretti et al. [8] to find the PS pixel. The result based on our analysis clearly shows LOS (Line of Sight) change in and around the focal area. We found the clear LOS change in the footwall and hanging wall side of the focal area. In the footwall side, the LOS is extended which may be subsidence or displaced to the westward. It is clear evidence of the viscoelastic relaxation after the mainshock pointed by [4, 5]. The hanging wall side LOS change is characteristic. In the hanging wall side, we found the two large amount LOS shortening regions. It is difficult to explain by the simple viscoelastic relaxation. It may be caused by long-term afterslip near the focal area, which may be triggered by the mainshock. Several scenes, however, might be affected by atmospheric and ionospheric disturbance. We need to reevaluate these effects for more accurate time series analysis.

[1] Miura et al., EPS, 2004, [2] Ohta et al., EPS, 2008, [3] Iinuma et al., GRL, 2009, [4] Ohzono, PhD dissertation, Tohoku Univ., 2009, [5] Ohta et al, JpGU Meeting, 2010, [6] Hooper et al., JGR, 2007, [7] Hooper et al., GRL, 2008, [8] Ferretti et al., IEEE Trans, 2001

Keywords: InSAR, 2008 Iwate-Miyagi Nairiku earthquake, StaMPS, ALOS/PALSAR, PS-InSAR, Crustal deformation

Quantitative comparison of methods and sensors for monitoring land subsidence based on SAR interferometric stacking

PASQUALI Paolo¹, RICCARDI Paolo¹, CANTONE Alessio¹, DEFILIPPI Marco¹, OGUSHI, Fumitaka^{2*}, GAGLIANO Stefano³

¹sarmap SA, ²Exelis VIS KK, ³Exelis Visual Information Solutions, Italia

Interferometric stacking techniques emerged in the last decade as methods to obtain very precise measurements of terrain displacements, and in particular subsidence phenomena. In particular, the so-called Persistent Scatterers (Ferretti et al. 2001) and Small BASeline (Berardino et al. 2002) methods can be considered as the two most representative stacking approaches. In both cases, the exploitation of 20 or more satellite Synthetic Aperture Radar (SAR) acquisitions obtained from the same satellite sensor with similar geometries on the interest area allows to measure displacements with an accuracy in the order of few mm / year, and to derive the full location history of good pixels with an accuracy of 1cm or better for every available date.

A main difference between the two approaches is the type of objects and land cover that are favoured in the analysis: the PS technique focuses on so-called Point Targets, i.e. objects possibly of small size and with a very well characterized geometry like corner reflectors (e.g. buildings, rocks) and with a high temporal stability of the backscattered signal; the SBAS technique vice-versa is concentrating the analysis on so-called distributed targets, like open fields and not very geometrically characterized objects.

The PS approach is then not making any assumption on spatial correlation of the displacement to be measured, but more on its linearity; the SBAS approach vice-versa is more robust in case of spatially correlated displacements, and allows in this case to monitor larger displacement rates. This paper is performing an extensive analysis and comparison of the results that have been obtained with the two approaches in a same geographical area in Japan, characterized by subsidence due to water and natural gas extraction.

The analysis is based on data acquired from the ALOS PALSAR (L-band), ENVISAT ASAR (C-band) and COSMO-SkyMed (X-band) satellite instruments, and the validation of the results is based on GPS and leveling measurements. The analysis allows to draw conclusions on pros and cons of the different approaches and sensors for deriving the displacement measures for monitoring subsidence phenomena. The feasibility of exploiting the same approach in different geographical areas is also discussed. Finally, comments are given on the outcomes of this analysis in view of the exploitation of the data to be available from the forthcoming Sentinel-1 (C-Band) and ALOS-2 (L-Band) missions.

REFERENCES

Ferretti, A., Prati, C., & Rocca, F. 2001: Permanent scatterers in SAR interferometry, IEEE Transactions on Geoscience and Remote Sensing, 39, 8-20.

Berardino, P., Fornaro, G., Lanari, R., & Sansosti, E. 2002: A new algorithm for surface deformation monitoring based on small baseline differential SAR interferograms, IEEE Transactions on Geoscience and Remote Sensing, 40, 2375- 2383.

Keywords: Synthetic Aperture Radar, Interferometry, Persistent Scatterers, Small BASeline, ALOS PALSAR

An Attempt to Increase Estimation Accuracy of Differential SAR Interferometry using Polarization

ISHITSUKA, kazuya^{1*}, TSUJI, Takeshi¹, Toshifumi Matsuoka¹

¹Graduate School of Engineering, Kyoto University

Differential SAR Interferometry (DInSAR) is a method to estimate surface displacement in line of sight direction between observations, which have provided us innovative insights into crustal movement. Although we estimate precious displacement using DInSAR analysis, the accuracy of results depends on the observation and surface conditions of the analyzed area. Here, we focus on the decorrelation as one of the main sources of measurement error. In the resolution-cell of vegetation and various scatters, the observed phase is not sometimes deterministic, resulting decorrelation. Thus, to decrease decorrelation area and improve the accuracy of estimation, we propose DInSAR analysis using polarimetric information.

Polarized wave is denoted by the combination of horizontal (H) and vertical (V) component. By using polarized wave, four SAR images (HH, HV, VH, VV) can be observed, where XY indicates polarization of observed (X) and transmitted (Y) wave. Since an arbitrary scatter condition can be obtained from these four images, we can estimate a scatter condition creating maximum coherence in the resolution cell (Cloude and Papathanassiou, 1998). In this study, we tried to estimate surface deformation from an optimized scatter condition. SAR images used in this study are observed by PALSAR instrument on Japanese satellite (ALOS) and covered with land subsidence area in Chiba prefecture. By using this analysis, we can reveal subsidence in the condition of better coherence.

Keywords: Differential SAR Interferometry, Polarization, Interferometric Coherence, Land Subsidence

Estimation of the area and the thickness of volcanic ash by using DInSAR technique

NAKANO, Youko^{1*}, SHIMIZU, Takeshi¹, YAMAKOSHI, Takao¹, Tadanori Ishizuka¹, Eiichi Wakabayashi²

¹Public Works Research Institute, ²Yachiyo Engineering CO., LTD.

On October 26, 2010, Mt. Merapi located in central Java Island in Indonesia erupted. This eruption caused a huge pyroclastic flow. And the Gendol River originating from the southern flank of Mt. Merapi, was filled with pyroclastic deposit. Lahars occurred on the rivers originating from the western flank of Mt. Merapi, during the rainy seasons from 2010 to 2012. The area of western flank of Mt. Merapi is assumed to have been covered with thick volcanic ash by the eruption. It is assumed that the thick volcanic ash caused a frequent occurrence of mudflows at the rivers located on western flank of Mt. Merapi.

On the other hand, Ozawa (2011) reported that the estimated thickness by the interferogram generated from a pair of the JAXA's ALOS/PALSAR images before and after eruption, was in good agreement with the result of field investigation of volcanic ash on the 2011 Mt. Kirishima (Shinmoe-peak) eruption.

The authors estimated the area and the thickness of volcanic ash at the time of the eruption of Mt. Merapi through the same technique and the same satellite sensor utilized by Ozawa (2011). And on the other hand, we conducted a field survey of the thickness of volcanic ash between Sept. 2011 and Feb. 2012. The authors earned that the estimated area and thickness of volcanic ash by DInSAR, was in good agreement with result of field investigation of volcanic ash.

ACKNOWLEDGMENT: The authors would like to thank JAXA for its free provision of ALOS imagery, and thank M. Shimada of JAXA for the use of his SIGMA-SAR interferometry software [M. Shimada, 1999].

Keywords: Mt. Merapi, volcanic ash, volcanic ash, DInSAR